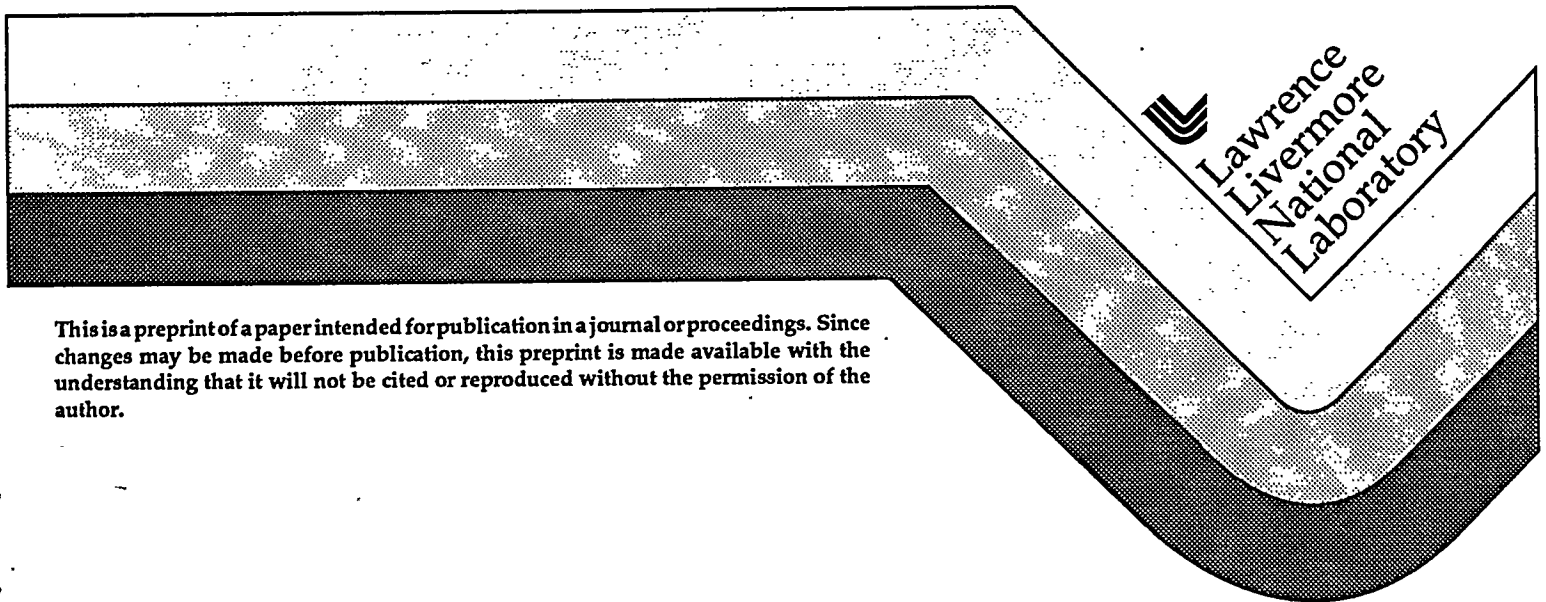# Atomistic Simulation of Point Defects and Dislocations in bbc Transition Metals from First Principles

W. Xu
J. A. Moriarty

RECEIVED
FEB 2 0 1996
OSTI

This paper was prepared for submittal to the
Workshop on Modeling of Industrial Materials
Santa Barbara, California
January 7-11, 1996

January 19, 1996

Lawrence Livermore National Laboratory

MASTER

DISCLAIMER

Atomistic Simulation of Point Defects and Dislocations in bcc Transition Metals from First Principles

Wei Xu and John A. Moriarty

Lawrence Livermore National Laboratory, University of California, Livermore, CA 94551

(January 5, 1996)

Abstract

Using multi-ion interatomic potentials derived from first-principles generalized pseudopotential theory, we have been studying point defects and dislocations in bcc transition metals, with molybdenum (Mo) as a prototype. For point defects in Mo, the calculated vacancy formation and activation energies are in excellent agreement with experimental results. The energetics of six self-interstitial configurations in Mo have also been investigated. The <110> split dumb-bell is found to have the lowest formation energy, as is experimentally observed, but the corresponding migration energy is calculated to be 3-15 times higher than previous theoretical estimates. The atomic structure and energetics of <111> screw dislocations in Mo are now being investigated. We have found that the "easy" core configuration has a lower formation energy than the "hard" one, consistent with previous theoretical studies. The former has a distinctive 3-fold symmetry with a spread out of the dislocation core along the <112> directions, an effect which is driven by the strong angular forces present in these metals.

61.72.Bb,61.72.Ji,61.72.Lk,62.20.Fe

It is very important to understand point-defect and dislocation properties at the atomistic level to develop larger length-scale theories of the mechanical properties of metals. In particular, accurate determinations of the atomic core structure and energetics of isolated dislocations is crucial for the understanding of the low-temperature plasticity of bcc metals. Although the rapid improvement and development of experimental tools in recent years, e.g., the scanning tunneling microscope (STM), the field ion microscope (FIM), the high resolution transmission electron microscope (HRTEM) etc., has significantly improved the prospects for directly observing the structures of crystal defects at the atomic level, many details of these structures remain beyond the scope of these tools. With the corresponding rapid development in high-performance computing capabilities and efficient numerical algorithms, however, atomistic simulations based on realistic physical models are becoming a powerful supplement to current experimental methods.

The accurate atomistic simulation of crystal defects in metals requires the use of appropriate interatomic potentials which take into account the electronic structure of the metal in a meaningful and systematic way. Most calculations of point defects and dislocations in metals [1–3] have used radial-force empirical potentials, including both pair potentials and many-body "glue" models such as Finnis-Sinclair (FS) potentials [4] and embedded-atom-method (EAM) potentials [5]. It has been recognized, however, that this is not adequate in general for the central bcc transition metals, as discussed by Carlsson [6] and others. Accurate atomistic simulations of point defects and dislocations in the bcc metals require the strong angular forces present in these materials which arise from multi-ion d-state interactions. In recent years, several interatomic potentials [7] based on tight-binding theory and explicitly containing angular-force contributions have been developed for bcc transition metals and applied successfully to study structural stability and surface properties. At the same time, Moriarty [8] has derived multi-ion interatomic potentials for transition metals from first-principles generalized pseudopotential theory (GPT). For atomistic simulations on the bcc metals, a simplified model GPT or MGPT has been developed using canonical d bands and which produces entirely analytic three- and four-ion potentials [9,10]. In the

2

case of molybdenum (Mo), MGPT potentials have been sucessfully applied to the cohesive, structural, elastic, vibrational, thermal, and melting properties of the bulk metal [10]. In this paper, we have applied the same MGPT potentials to study vacancies, interstitials, and <111> screw dislocations in Mo. We intend this work to serve as a preliminary first step for future studies on dislocation motion in bcc metal systems, including the calculation of the Peierls barrier and its environmental dependence.

The point defects studied here, i.e., the single vacancy and interstitial, are modeled within a large cubic cell to which periodic boundary conditions are applied in all three directions. The conjugate gradient method [11] is used to determine the stable structures through energy minimization. To calculate the migration energy barrier, we march one atom, which is the interstitial atom or the nearest neighbor atom in the vacancy case, from its equilibrium site towards another nearest equilibrium or vacancy site. During the migration process, we allow the migrating atom to relax in the plane perpendicular to the vector between its initial and final positions. This ensures finding the minimum (optimal) energy path for migration. Meanwhile, all other atoms are fully relaxed, except for one atom on the corner of cell which is frozen to prevent a rigid shift of the simulation cell behind the "marching" atom. One stationary point (maximum) is found and it corresponds to the migration atom at the saddle point (E_{saddle}). The migration energy E^m is given by:

$$E^m = E_{saddle} - E_{min.} \tag{1}$$

Using MGPT interatomic potentials, we have calculated the formation and migration energies of a single Mo vacancy. A cell of size $5a \times 5a \times 5a$, where a is lattice constant of Mo, was created with a total of 249 atoms plus one vacancy in the center. The calculation was carried out at 0 K and constrained with a constant volume condition. In Table I we list the unrelaxed and relaxed vacancy formation energy, E_v^f, that we obtain for Mo. Compared with the unrelaxed value, the relaxed formation energy is about 4% lower and in excellent agreement with experimental result measured by Maier et al. [12]. In order to check any size effect of the simulation cell on the result, a larger cell with 685 total atoms has also

3

been used. We found that the formation energy is almost identical to that of 249-atom cell (<1% difference). In the calculation of the vacancy migration energy, E_v^m, we constrained the migrating atom, a nearest neighbor of the vacancy, to lie on a particular plane which is perpendicular to the migration path along <111>. As indicated in Table I, our calculated migration energy for Mo is 1.6 eV. Experimentally, only the activation energy, Q_v, which is the sum of vacancy formation and migration energies, can be measured. Using our calculated values of E_v^f and E_v^m, we find that the activation energy Q_v is 4.5 eV for Mo, in excellent agreement with the measured result.

We have carried out MGPT calculations on Mo self-interstitials for the various possible symmetry positions in a bcc structure. Six different configurations have been considered which include octahedral, tetrahedral, and crowdion sites, and split dumb-bell sites along the <100>, <110> and <111> directions. All six configurations are metastable and the calculated equilibrium positions are given in Table II. Due to the large strain fields generated by such interstitial defects, it is important to check the convergence of the formation energy, E_i^f, with respect to cell size in constant volume calculations. Based on a detailed test, we have chosen a 1024-atom cell to use in all our calculations. The resulting formation energies for the six interstitial configurations are listed in Table II. We find the <110> split dumb-bell to have the lowest formation energy, $E_i^f = 10.9$ eV at $\pm(0.26, 0.26, 0.0)a$, in agreement with the configuration found by X-ray diffuse scattering measurements [13]. Table II also lists the results on self-interstitial formation energies in Mo calculated by Harder and Bacon using the original Finnis-Sinclair potential [2], denoted as FS(1). Obviously, MGPT yields much higher values than FS(1), and this is a direct reflection of the strong angular forces present in the former potentials, which disfavor non-bcc angles.

An asymmetric metastable configuration at $\pm(0.3182, 0.1958, 0.0182)a$, which is rotated from the <110> dumb-bell position $\pm(0.26, 0.26, 0.0)a$, has been reported previously with the lowest formation energy by Thetford [14] using a modified Finnis-Sinclair potential, FS(2). To check this so-called bent configuration, we also broke the symmetry of <110> dumb-bell and relaxed the structure. However, our calculations revealed that the bent

4

interstitial is an unstable configuration which will eventually return to the original <110> dumb-bell position.

We have studied three migration paths for an <110> split dumb-bell interstitial migrating along <111> directions (Fig. 1). Paths A and B involve migrations of the dumb-bell center to one of its nearest neighbor sites along <111> with a jump length $\sqrt{3}/2a$. The difference between paths A and path B is that the orientation of the dumb-bell will rotate to another <110> direction in path B, while it will remain the same in path A. In path C the dumb-bell will not change its orientation, only the center will make a double jump along <111>. As shown in Table III, we calculate that path B possesses the lowest migration energy barrier in Mo (0.76 eV). At the same time, the magnitudes of the MGPT migration energies are 3-15 times higher than previous theoretical estimates obtained using simple radial-force Finnis-Sinclair potentials for Mo [2,3].

In calculating the structure of a <111> screw dislocation, we construct a slab with the z direction parallel to the burgers vector b, which is along <111>. The x and y directions are chosen along <112> and <110>, respectively (see Fig. 2). Periodic boundary conditions are applied in the z direction only, in order to simulate an infinite dislocation. In the x and y directions, we use a fixed boundary condition. In doing so, we further divide the system into two regions: an inner region and an outer region. The dislocation core is contained in the inner region where atomic positions are fully relaxed. The outer region surrounds the inner region and in it atomic positions are fixed according to the initial displacements generated by anisotropic elasticity theory [15]. Simulation cells with different sizes ranging from 600 atoms up to 2160 atoms have been used in the calculation. Due to a large distortion caused by the dislocation, a large simulation cell is required to yield a stable core. We here present results obtained from a 1946-atom cell with 1074 atoms in the inner region.

Two core configurations in bcc Mo have been considered. The first one is the so-called "easy" core <111> screw dislocation with the burgers vector in the positive z direction. In this configuration, the stacking sequence of the three neighboring [111] atom rows which are closest to the core center is preserved but reversed in sense (see Fig. 2). The second

5

configuration we have considered is so-called "hard" core <111> screw dislocation. This configuration has its burgers vector in the opposite direction to the "easy" one, with both dislocation centers located on the same site. The stacking sequence of the three atom rows surrounding the core center is destroyed in the "hard" configuration and those three atoms always lie in the same {111} plane. Using the MGPT potentials, we have found that the "easy" core configuration in Mo has a lower formation energy than the "hard" one, which is consistent with general expectations as well as previous theoretical studies [1,16]. We have also found that all inner region atoms are relaxed in all three directions, especially the x and y directions. The magnitude for the largest in-plane relaxation is about one tenth of the burgers vector.

The differential displacement (DD) method [1] has been used to elaborate the detailed characteristics of the dislocation core configurations. In the DD method the <111> component of the relative displacement of neighboring atoms due to the dislocation (i.e., the total relative displacement less than that in the perfect lattice) is drawn as an arrow between the corresponding atoms. For each atom the differential displacements of the six nearest neighbor atoms in the <111> projection, corresponding thus to the <111> displacements in the three {110} planes (i.e., along 3 <112> directions) of the <111> zone, can be shown. The DD map for the MGPT "hard" core configuration is very similar to that of the non-degenerate core calculated by the tight-binding recursion method [16] which in turn is also very similar to the DD map generated from anisotropic elasticity theory. The DD map of MGPT "easy" core, on the other hand, is much different compared with that of anisotropic elasticity theory. Substantial rearrangement occurs after the core region is fully relaxed. The high symmetry of the anisotropic-elastic core is broken and a 3-fold symmetric core which spreads out along the three <112> directions is obtained, as illustrated in Fig. 3. The 3-fold symmetry of the core extensions is reminiscent of Hirsch's early suggestion of a 3-fold dissociation of the core into three partial dislocations. Such a conclusion was also reached in earlier theoretical studies [1,17].

One significant question is raised from these calculations: why does the "easy" <111>

screw dislocation spread out along three <112> directions? A simple argument which is based on tracking the change of nearest neighbor (NN) bond lengths and bond angles has been developed to help answer this complicated question. A detailed comparison has been made between the bond lengths and bond angles of the anisotropic-elastic dislocation core (without spread out) and the MGPT dislocation core (with spread out). For the three atoms surrounding the dislocation center, we have found that all of their NN bond lengths except one are closer to the bcc value in the MGPT core. Most importantly, the NN bond angles are found to be closer to those of the bulk bcc structure when the dislocation spreads out along the three <112> directions. This is a reflection of the strong MGPT angular forces which favor the bcc bond angles. Thus it is energetically favorable for an "easy" <111> screw dislocation to be spread out in such a way as to restore the bulk-like structure.

In summary, we have systematically studied vacancies, self-interstitials, and <111> screw dislocations in the bcc transition metal Mo, using multi-ion interatomic potentials derived from first-principles generalized pseudopotential theory. The calculated vacancy formation and activation energies are in excellent agreement with experimental results. The <110> split dumb-bell interstitial is found to have the lowest formation energy, also in agreemment with experiment, and with a calculated migration energy 3-15 times larger than previous theoretical estimates. The atomic structures of <111> screw dislocations in Mo have been investigated, and it is found that the stable dislocation core structure involves spread out along the three <112> directions. A simple argument based on bond coordination and bond angles has been proposed to explain this spread out. In the future, we intend to extend this work to the study of dislocation energetics, including the calculation of the Peierls barrier, and to treat additional bcc metals such as tantalum.

REFERENCES

[1] V. Vitek, Crystal Lattice Defects **5**, 1 (1974) and references therein.

[2] J. M. Harder and D. J. Bacon, Phil. Mag. A. **54**, 651 (1986).

[3] R. Thetford, in *Many-Atom Interactions in Solids*, edited by R. M. Nieminen, M. J. Puska, and M. J. Manninen (Springer-Verlag, Berlin, 1990), p. 176.

[4] M. W. Finnis and J. E. Sinclair, Phil. Mag. A, **50**, 45 (1984).

[5] M. S. Daw and M. I. Baskes, Phys. Rev. Lett. **50**, 1285 (1983); Phys. Rev. B **29**, 6443 (1984); S. M. Foiles, M. S. Daw, and M. I. Baskes, Phys. Rev. B **33**, 7983 (1986).

[6] A. E. Carlsson, in *Solid State Physics: Advances in Research and Applications*, Vol. **43**, edited by H. Ehrenreich and D. Turnbull (Academic Press, Boston, 1990), p. 1.

[7] A. E. Carlsson, Phys. Rev. B **44**, 6590 (1991); D. G. Pettifor, Phys. Rev. Lett. **63**, 2480 (1989); S. M. Foiles, Phys. Rev. B **48**, 4287 (1993); W. Xu and J. B. Adams, Surf. Sci. **301**, 371 (1994).

[8] J. A. Moriarty, Phys. Rev. **38**, 3199 (1988).

[9] J. A. Moriarty, Phys. Rev. **42**, 1609 (1990).

[10] J. A. Moriarty, Phys. Rev. **49**, 12431 (1994).

[11] *Numerical Recipes in Fortran*, eds. W.H. Press *et al.*, (Cambridge Press, 1992).

[12] K. Maier, M. Peo, B. Saile, H. E. Schaefer, and A. Seeger, Phil. Mag. A, **40**, 701 (1979).

[13] P. Erhart, J. Nucl. Mater., **69**, 200 (1978).

[14] R. Thetford, AERE report No. M3507 (Harwell: Atomic Energy Research Establishment).

[15] J. D. Eshelby, W. T. Read, W. Shockley, Acta Met. **1**, 251 (1953); A. N. Stroh, Phil. Mag. **3**, 625 (1958); A. K. Head, Phys. Stat. Sol. **6**, 461 (1964); J. P. Hirth and J. Lothe,

Phys. Stat. Sol. **15**, 487 (1966).

[16] K. Kimura, S. Takeuchi, and K. Masuda-Jindo, Phil. Mag. A **60**, 667 (1989).

[17] . M. S. Duesbury, Contemp. Phys. **27**, 145 (1986).

TABLES

TABLE I. Single vacancy formation energy E_v^f, migration energy E_v^m, and activation energy Q_v for Mo, in eV.

	MGPT	Experiment[a]
E_v^f(unrelaxed)	3.0	
E_v^f(relaxed)	2.9	3.0 ($\pm$ 0.3)
E_v^m	1.6	
Q_v	4.5	4.5 ($\pm$ 0.3)

[a] Reference [12].

TABLE II. Self-interstitial formation energies of six interstitial sites for Mo, in eV.

Interstitial configuration	Position in bcc lattice	E_i^f	
		MGPT	FS(1)[a]
<110> split dumb-bell	$\pm(0.26, 0.26, 0.00)a$	10.9	7.0
crowdion	$(0.25, 0.25, 0.25)a$	13.9	7.2
<111> split dumb-bell	$\pm(0.22, 0.22, -0.22)a$	14.2	7.3
tetrahedral	$(0.50, 0.25, 0.00)a$	14.9	7.6
<100> split dumb-bell	$\pm(0.38, 0.00, 0.00)a$	16.3	7.2
octahedral	$(0.50, 0.50, 0.00)a$	17.5	7.6

[a] Reference [2].

TABLE III. Migration energies for the <110> split dumb-bell interstitial for Mo, in eV.

Path of migration	E_i^m		
	MGPT	FS(1)[a]	FS(2)[b]
A: parallel jump	2.52	0.18	0.25
B: jump + rotation	0.76	0.16	0.23
C: 2 parallel jumps	2.12	0.24	

[a] Reference [2]. [b] Reference [3].

11

FIGURES

FIG. 1. Schematic of self-migration paths (A, B and C) for the <110> split dumb-bell interstitial.

FIG. 2. Top view and side view of the <111> screw dislocation in Mo. Side views are only two rows of atoms which contain the dislocation center (dash line region in top view).

FIG. 3. The <111> projection of the differential displacement (DD) map of the "easy" core configuration from a) anisotropic elasticity theory and b) MGPT interatomic potentials.
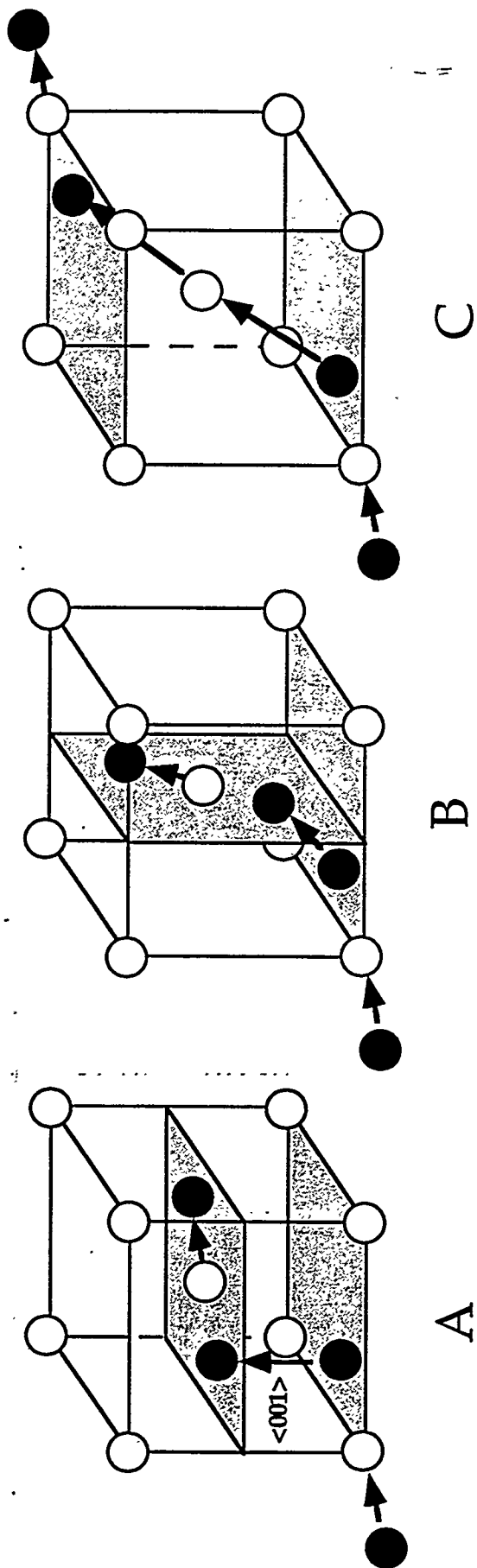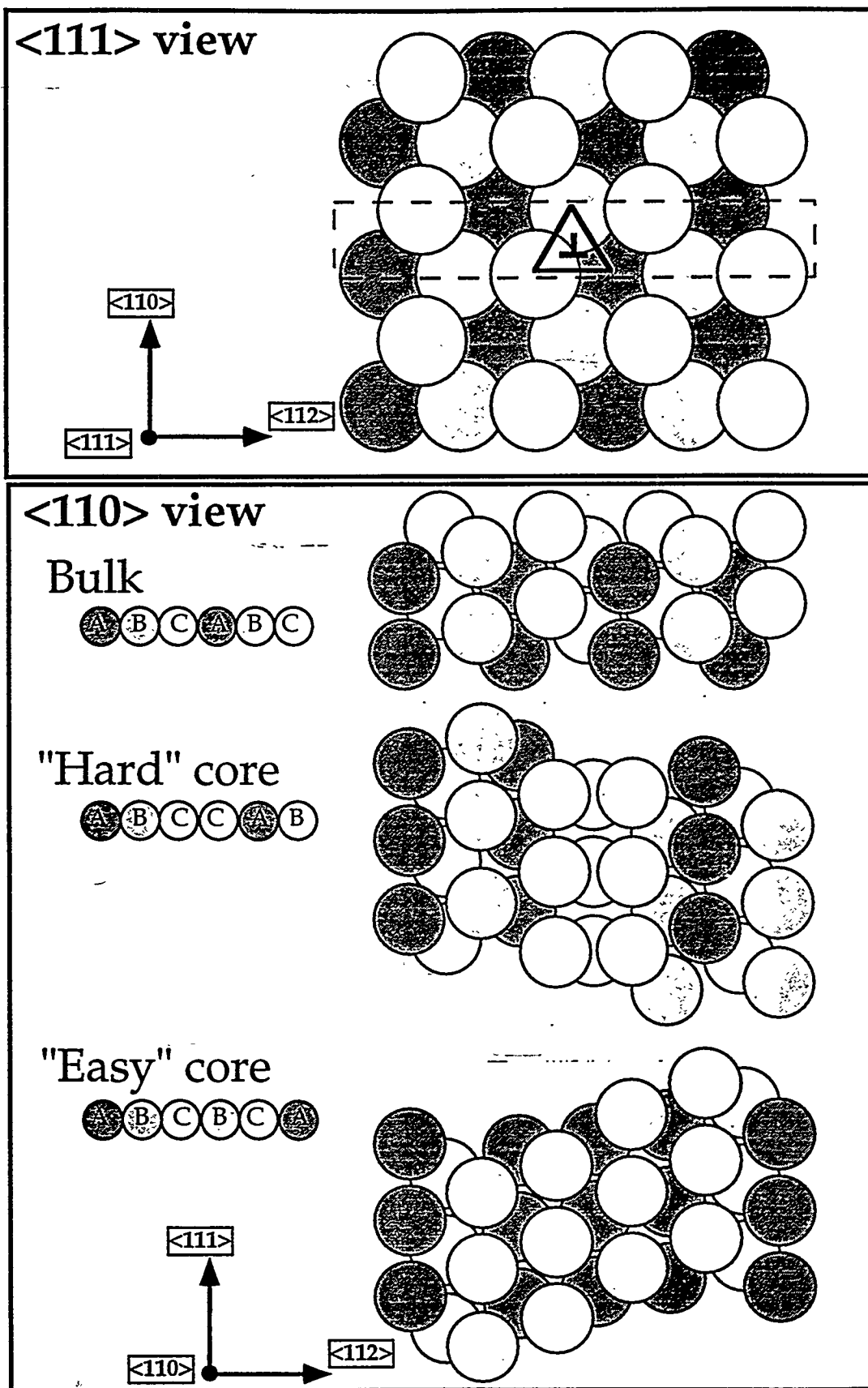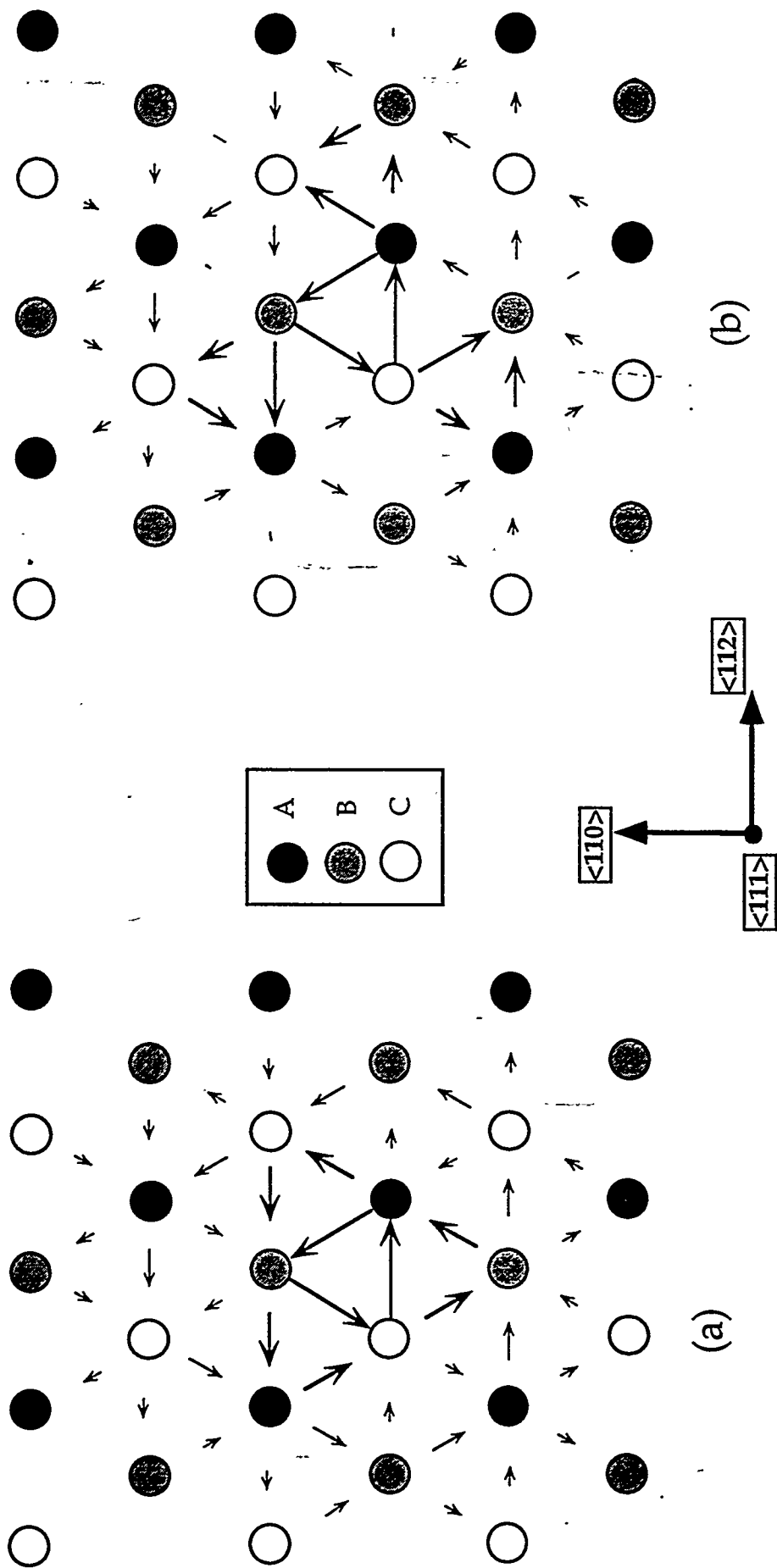
<001>

A   B   C

Fig. 1.

<111> view

<110>

<112>

<111>

<110> view

Bulk

Ⓐ Ⓑ Ⓒ Ⓐ Ⓑ Ⓒ

"Hard" core

Ⓐ Ⓑ Ⓒ Ⓒ Ⓐ Ⓑ

"Easy" core

Ⓐ Ⓑ Ⓒ Ⓑ Ⓒ Ⓐ

<111>

<110>

<112>

FIG. 2.

(b)

(a)

A	●
B	◉
C	○

<110>
<112>
<111>

FIG. 3.